LA-UR- 08-7512

Approved for public release;
distribution is unlimited.

Title:	Chaos and Structure of Level Densities
Author(s):	Sven Aberg and Henrik Uhrenholt, Lund University Takatoshi Ichikawa, RIKEN Peter Moller, T-2
Intended for:	International Journal of Modern Physics E

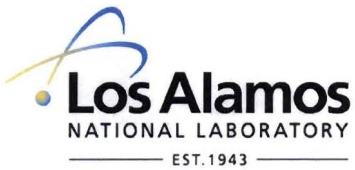

Form 836 (7/06)

CHAOS AND STRUCTURE OF LEVEL DENSITIES

SVEN ÅBERG and HENRIK UHRENHOLT

Mathematical Physics, LTH, Lund University, P.O. Box 118, S-221 00 Lund, Sweden

TAKATOSHI ICHIKAWA

RIKEN Nishina Center, RIKEN, Wako, Saitama 351-0198, Japan

PETER MÖLLER

Theoretical Division, Los Alamos National Laboratory, Los Alamos, New Mexico 87545, USA

Two coexisting facets of warm nuclei, quantum chaos and structure of the level density, are considered. A newly developed combinatorial level-density model is presented, and the role of collective enhancements discussed. An example of extreme parity enhancement is shown.

1. Introduction

The energy region of the first few MeV above the ground state shows interesting features of the nucleus. Beyond an ordered energy region just above the ground-state the dynamics changes, and chaotic features are observed in the neutron resonance region. The statistical properties of energies and wave-functions are common to all chaotic nuclei. However, if instead a global property, like the local level-density function is studied, strong structure effects emerge. In this contribution we discuss these two different facets of *warm nuclei.*

In section 2 the onset of chaos with increasing excitation energy is discussed, with both experimental observations and proposed theoretical mechanisms as starting points. The structure of level densities in the same excitation energy region based on the two different starting points, is treated in section 3, where we give a short presentation of a newly developed combinatorial level-density model[1]. Some results from the model are presented and discussed.

2. Quantum Chaos in the Nucleus

The famous conjecture by Bohigas et al[2] states that *Energies and wave functions for a quantum version of a classically chaotic system show generic statistical behavior described by random matrix theory.* Classically regular systems follow Poisson statistics while classically chaotic systems follow statistics of Gaussian Orthogonal

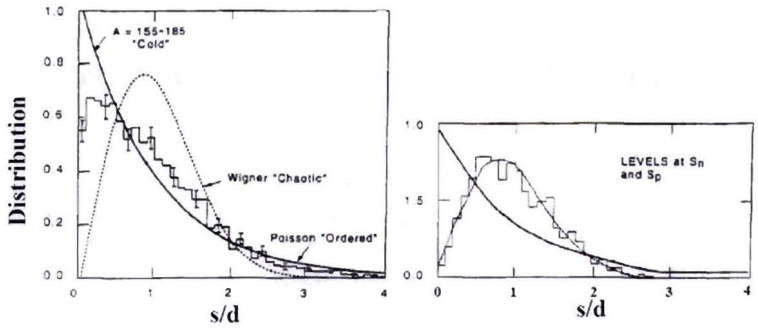

Fig. 1. Nearest-neighbor spacing distributions from experimental data. The left-hand figure shows the near-yrast region, and the right-part figure the neutron resonance region. From Ref.[3].

Ensembles, GOE (if time-reversal invariant) in the corresponding quantum versions. Consequently, the term *quantum chaos* is used to describe quantum systems that in the classical limit are chaotic. Although it is difficult to speak about a classical correspondence to the nuclear many-body problem, the term *quantum chaos* is often used as a characterization of a quantum system that exhibits statistical features from GOE, and in this contribution we shall follow this practice.

In Fig. 1 the experimental information for heavy nuclei clearly shows that cold states, close to the ground state (or the yrast line), exhibit a nearest-neighbor distribution of Poisson statistics, characteristic of regular dynamics (left-hand figure), while states in the neutron resonance region at 7-8 MeV show chaotic features, i.e. follow GOE statistics (right-hand figure). Thus, a transition from order to chaos appears somewhere in the energy region between 0-8 MeV. The transition point can be studied theoretically in a model that mixes many-body wave-functions through a residual two-body interaction.

In Refs.[4,5] the many-body states (Slater determinants) are described as n-particle-n-hole excitations of the deformed and rotating many-body ground state, $|0>$,

$$|\mu>=\prod_{i=1}^{n} a^{+}_{m_i} a_{j_i}|0>, \tag{1}$$

where all configurations with n=1, 2, 3 ... are considered. The corresponding energy is given as,

$$E_\mu = \sum_{i=1}^{n} (\varepsilon_{m_i} - \varepsilon_{j_i}) + E_0, \tag{2}$$

where E_0 is the ground-state energy, ε are eigen energies to the one-body deformed (and rotating) mean field Hamiltonian, and the indices m and j refer to particle

and hole states, respectively. A residual two-body interaction, $\hat{W}$, is subsequently added and the total many-body Hamiltonian is written as,

$$\hat{H} = \sum_i \varepsilon_i a_i^+ a_i + \frac{1}{4} \sum_{ijkl} W_{ijkl} a_i^+ a_j^+ a_k a_l, \tag{3}$$

where W_{ijkl} are two-body matrix elements of $\hat{W}$. Many-body energies and wave functions of the interacting many-body system are finally obtained by diagonalization in a truncated many-body space, giving eigen functions

$$|\alpha> = \sum_\mu c_{\alpha\mu} |\mu> . \tag{4}$$

This mixture of states is due to the residual interaction $\hat{W}$, and can be characterized by a spreading width, Γ_μ, that describes the energy range in which states are coupled. The size of the spreading width may be estimated from Fermis golden rule,

$$\Gamma_\mu = 2\pi \left\langle \bar{W} \right\rangle \rho_{2\mathrm{p}-2\mathrm{h}}(E_{\mathrm{exc}}), \tag{5}$$

where $\rho_{2\mathrm{p}-2\mathrm{h}}$ is the density of states at excitation energy E_{exc} that are directly coupled by the two-body residual interaction $\hat{W}$. The role of the residual interaction increases with increasing excitation energy, and chaos is found to set in[6] when the condition $\bar{W} \approx (\frac{1}{2} - \frac{1}{3})/\bar{\rho}_{2\mathrm{p}-2\mathrm{h}}$ is met. Based on microscopic calculations utilizing a δ-type two-body interaction with appropriate strength, it is found that chaos appears at about 3 MeV excitation energy for medium-heavy (rotating) nuclei[5].

3. Structure of the Level Densities

As discussed above, the chaotic features of the nucleus are theoretically suggested to set in already at about 3 MeV excitation energy in medium mass nuclei, and chaos is experimentally verified at the neutron separation energy. The chaoticity implies similar behavior of all nuclei concerning fluctuation properties. However, strong structure effects are present in other observables, as is seen in Fig. 2 where we show experimental level densities at the neutron separation energy, or more specifically, the inverse $1/D$ of the mean spacing of observed resonances (data from[7]). Strong shell effects with deep minima appear at shell closures, corresponding to neutron numbers, N=50, 82 and 126. The observed level density varies by more than six orders of magnitude. There is also a general increase of the level density with increasing mass number: on the average one expects that the level density is proportional the mass number A.

A new microscopic model for the level-density function is presented in[1]. Here we discuss some new results from this extensive study. In a similar way as discussed above, excited states are calculated as many-particle-many-hole excitations in the deformed mean field, with wave functions and energies given by Eqs.(1) and (2). The deformed mean field is obtained from[8], where all parameters, including

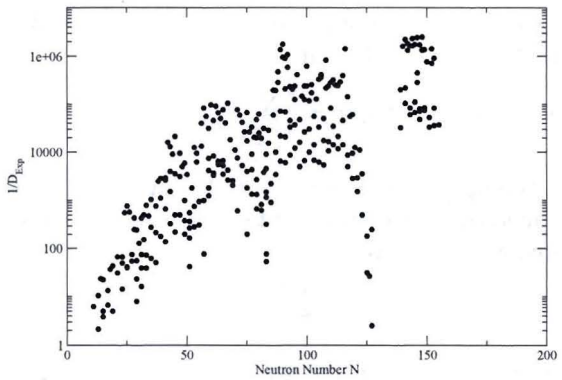

Fig. 2. Experimental level density at the neutron separation energy plotted as a function of the neutron number.

equilibrium deformations, are given. All np-nh states with $n < 10$ are included for protons as well as for neutrons, which are then combined to form total many-body states and ordered in energy. Pairing is included by performing a blocked BCS calculation for each many-body state, which provides a unique pairing gap for each state. This allows us, for example, to study either individual or average pairing gaps as functions of excitation energy[1]. In this model each state is specified by the energy, $E_\mu = E_\mu(v, K, \pi, \Delta_\mathrm{n}, \Delta_\mathrm{p})$ (corrected for the pairing interaction), the seniority (v=v_p+v_n), the K quantum number, the parity and the pairing gaps (cf. Eq.(2)).

To show how the level density is built up from the many-particle-many-hole excitations, we show in Fig. 3 the level density for seniorities, v=2, 4, 6 and 8, as functions of excitation energy. The figure is plotted in log-log scale. A significant result is that the different seniority level densities depend on excitation energy as, $\rho_v \propto E_\mathrm{exc}^{\alpha_v}$. The powers α_v are systematically larger than the estimate from the Fermi-gas model, $\alpha_v = v - 1$, namely rather like $\alpha_v = 1.6v - 1$. The difference can be understood from, on the average, larger energy distances in the s.p. spectrum around the Fermi surface than for states away from the Fermi surface (cf. Ref.[9]).

All states have been calculated as excitations in the mean field Hamiltonian. The ground-state deformation is assumed for all states, while the pair gaps are calculated self-consistently. As discussed in section 2 the residual interaction plays a most important role as the main cause of quantum chaos in the many-body system. In calculating the level-density function the residual interaction may be included as well. We shall consider two consequences of inclusion of the residual interaction. The first arises when we follow the lines described in section 2. A generic residual interaction creates a mixture of many-body states (Eq.(4)) on some energy scale and may cause chaos. This part of the interaction is not expected to create any structural changes, but its role is mainly to smear out the individual character of many-body wave functions and energies on some energy scale. The effects from the interaction

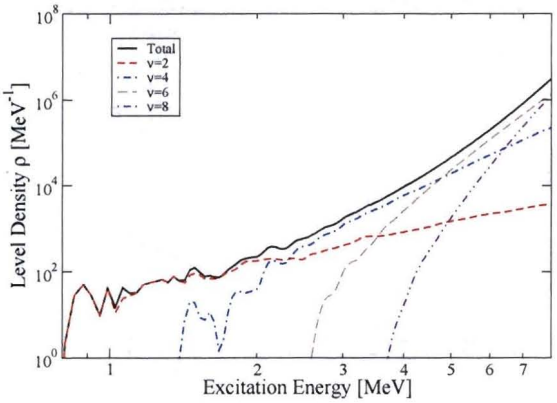

Fig. 3. Seniority level-density functions for ^{172}Yb (log-log scale) for v=2 (short-dashed line), 4 (dot-dashed line), 6 (long-dashed line) and 8 (dot-dot-dashed line). The total level density is shown as a thick, solid line.

can thus be taken into account by simply assuming that each state is smeared out with a damping with given by Eq.(5), that is estimated as[16] $\Gamma_\mu = 0.05 E_{\rm exc}^{3/2}/\sqrt{A}$ MeV.

Inclusion of long-range interactions provides the second consequence of the residual two-body interaction. This gives rise to vibrational excitations, including giant resonances, and we shall consider effects on the level density from a residual quadrupole interaction. This interaction gives rise to specific vibrational correlations, and provides a microscopic approach to the calculation of vibrational enhancements of the level density. Energies and wave functions of the phonons are obtained by solving the quasi-particle Tamm-Dancoff equations (QTDA) for *each* calculated state, see Ref.[1]. At present, we include quadrupole phonons only and assume a separable QQ-interaction where operators and coupling constants are chosen from the self consistency conditions[10]. The two Tamm-Dancoff equations corresponding to β- (K=0) and γ-vibrations (K=2) are solved. To the level-density function we thus add the quadrupole vibrational states (phonons) built on each many-body state, properly accounting for angular momentum coupling. In order not to double-count levels, qp-states building up the phonons are removed from the level-density function, with a weight given by the wave function component. By comparing level-density functions obtained with and without the inclusion of quadrupole phonons, we obtain a microscopic measure of the vibrational enhancement. In Fig. 4 the vibrational enhancement is shown versus excitation energy for ^{172}Yb. The effect is completely ignorable. And considerably smaller than the vibrational enhancement in the attenuated phonon model[12] (inset in Fig. 4), that is commonly employed in level-density calculations, see e.g. Ref[13]. Systematically, the vibrational enhancement factor around the neutron separation energy varies be-

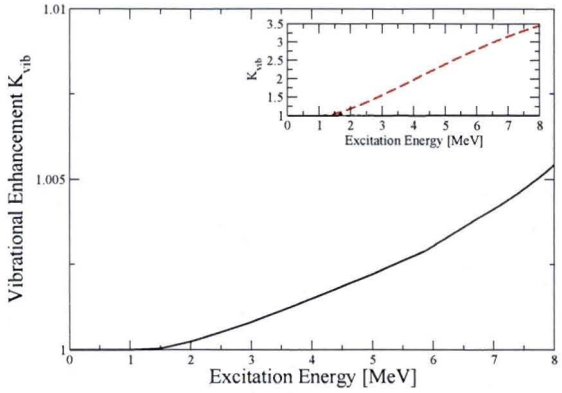

Fig. 4. Microscopically calculated vibrational enhancement for ^{172}Yb. The inset shows vibrational enhancement from the attenuated phonon model[12].

tween 1 and 1.2 in the present approach[1]. The reason why the effect is so small is the way the wave functions of the phonons are constructed. In the QTDA the phonon states are built as sums of correlated particle-hole excitations. While phonons corresponding to the giant resonances obtain strength from states with ph-energies quite different from the phonon energy, the wave-functions of the low-lying vibrational states consist of ph-components which are fairly close in energy to the energy of the phonon state. Therefore, the increase in level density obtained by including the phonons is small.

In addition, in the present approach the calculated quadrupole phonons are not allowed to be repeated. On the other hand, in the attenuated phonon model quadrupole (and octupole) phonons are treated as non-interacting phonons that are allowed to be repeated several times. Clearly, such an approach may give rise to problems with the Pauli principle, and may imply a double counting of states.

Deformed nuclei can rotate. We explicitly include this excitation mode in the model. In building rotational states we employ the calculated equilibrium deformation, and pairing gaps through the moment of inertia function, $J(\varepsilon, \Delta_{\rm p}, \Delta{\rm n})$. The moment of inertia is calculated from a simple schematic expression[14] that depends on the pairing gaps as well as on the deformation. Consequently rotational band is built on each calculated (bandhead) state, $E_\mu(v, K, \pi, \Delta{\rm n}, \Delta_{\rm p})$ that has a specified K-quantum number and parity, and with the moment of inertia depending from the calculated pairing gaps. The energy of this band is simply taken from the deformed-rotor model,

$$E_{rot}(I, K, \pi) = \frac{I(I+1) - K^2}{2J(\varepsilon, \Delta_{\rm p}, \Delta{\rm n})} + E_\mu, \tag{6}$$

where I is the total angular momentum and E_μ is the bandhead energy. This way of including rotation certainly contains an element of double counting levels. At the

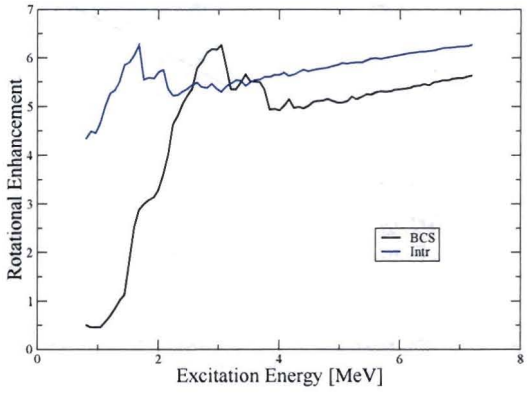

Fig. 5. Rotational enhancement of level density of ^{162}Dy. The upper curve shows the enhancement if pairing is neglected.

excitation energies considered here (up to the neutron resonance region) we believe, however this effect to be small[15].

The effect of including rotational states on the level-density function is shown in Fig. 5. At low excitation energies, $E_x < 3$ MeV, the rotational enhancement increases rather drastically, while a smaller increase is seen for higher excitation energies. At the neutron separation energy the rotational enhancement factor is in the range 5–6 for ^{162}Dy. If pairing is neglected all moments of inertia are described by the rigid-body value and energies are not pairing correlated. In general this implies a slightly larger rotational enhancement, with the largest effect at low excitation energies.

The level-density function as a function of the excitation energy, from the ground-state region to the neutron resonance region, has been measured for a few nuclei[17]. In Fig. 6 measured and calculated level-density functions are compared for ^{172}Yb. The agreement is good, in particular considering that no model parameters are fitted to experiment. We also show effects on the total level density if rotations/vibrations are excluded, or if pairing is excluded.

In the Fermi-gas model the positive and negative parities have the same density of states, $R = \rho_-(E_x)/\rho_+(E_x) = 1$. In Fig. 7 the level-density functions for negative and positive parities, as obtained from the microscopic combinatorial method, are shown versus excitation energy for the nucleus ^{79}Cu. The negative-parity states completely dominate the level density up to about 15 MeV. In fact, the ratio reaches values of about $R \approx 100$ at around 5 MeV excitation energy!

The isotope ^{79}Cu has a quite large neutron-proton ratio with $N = 50$ neutrons

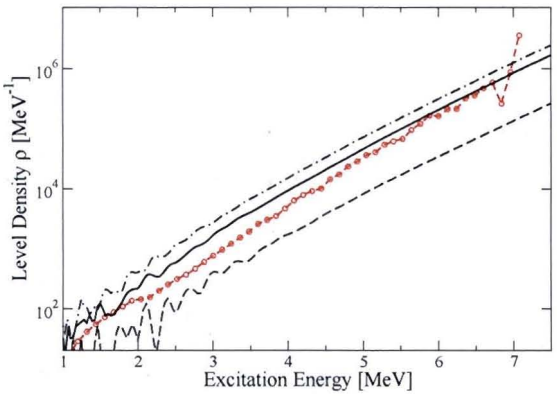

Fig. 6. Level density for ^{172}Yb as obtained in the microscopic model (solid line) is compared to experimental data from the Oslo group[17] (circles connected by lines). Excluding pairing (dot-dashed line) overestimates the level density, while excluding collective enhancements (rotations and vibrations), shown by a dashed line, gives underestimates of the level density.

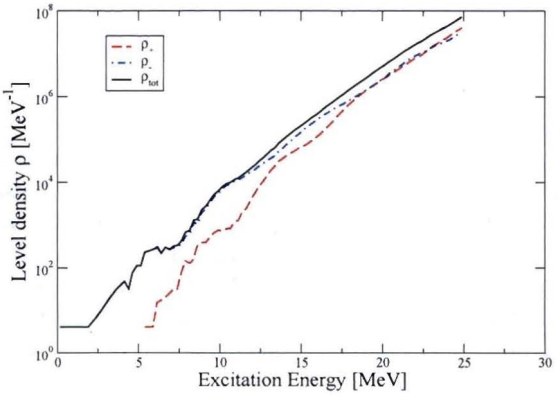

Fig. 7. Total level density for ^{79}Cu and the positive and negative parity components.

and $Z = 29$ protons. Due to the neutron number, which corresponds to a magic number, and a proton number being just one particle beyond the $Z = 28$ shell closure, the nucleus has almost spherical shape, $\varepsilon = 0.05$. Below the $N = 50$ gap is the $g_{9/2}$ shell and just above are the $g_{7/2}$ and $d_{5/2}$ shells, which all have positive parity. Consequently, most neutron excitations will keep the parity unchanged. The proton Fermi surface is in the center of the fp-shell with j-shells corresponding to negative parity, and most proton excitations will remain in the fp-shell, where the odd particle determines the parity as negative. This implies that most excited states of the combined system have negative parity, explaining the huge size of the

enhancement of negative parity in the level density. Not until we reach excitation energies of about 20 MeV will the parity ratio approach the normal, $R \approx 1$.

References

1. H. Uhrenholt, S. Åberg, P. Möller, and T. Ichikawa, to be publ.
2. O. Bohigas, M. Giannoni and C. Schmit, Phys. Rev. Lett. **52**, 1 (1984).
3. J.D. Garrett, J.Q. Robinson, A.J. Foglia and H.-Q. Jin, Phys. Lett. **B392**, 24 (1997).
4. S. Åberg, Phys. Rev. Lett. **84** 3119 (1990).
5. M. Matsuo, T. Døssing, E. Vigezzi, and S. Åberg, Nucl. Phys, **A620**, 296 (1997).
6. S. Åberg, Prog. Part. Nuc. Phys., Vol.28, 11 (1992).
7. RIPL2, Reference Input Parameter Library, IAEA-Tecdoc, 2005, http://www-nds.iaea.or.at/ripl2.
8. P. Möller, J. R. Nix, W. D. Myers, and W. J. Swiatecki, At. Data and Nucl. Data Tables **59** (1995) 185.
9. S. Åberg, Nucl. Phys. **A477** 18 (1988).
10. H. Sakamoto and T. Kishimoto, Nucl. Phys. **A501**, 205 (1989); S. Åberg, Phys. Lett. **B157**, 9 (1985).
11. S. Åberg, Nucl. Phys. **477**, 18 (1988).
12. A.V. Ignatyyuk et al, Phys. Rev. **C47** 1504 (1993).
13. S. Hilaire and S. Goriely, Nucl. Phys. **A779** 63 (2006).
14. R. Bengtsson and S. Åberg, Phys. Lett. **B172**, 277 (1986).
15. S. Bjørnholm, Aa. Bohr and B.R. Mottelson, *Physics and Chemistry of Fission*, Proc. Conf. Rochester (IAEA, Vienna), Vol.1 p.367 (1974).
16. B. Lauritzen, Th. Døssing and R.A. Broglia, Nucl. Phys. **A457**, 61 (1986).
17. A. Schiller et al, Nucl. Instr. Meth. Phys. Res. **A447** 498 (2000); A. Schiller et al, Phys. Rev. **C63**, 021306(R) (2001)